

Highly tunable spin-dependent electron transport through carbon atomic chains connecting two zigzag graphene nanoribbons

Yuehua Xu,¹ Bao-Ji Wang,¹ and San-Huang Ke^{1,2,*}

¹Key Laboratory of Advanced Microstructured Materials, MOE, Department of Physics, Tongji University, 1239 Siping Road, Shanghai 200092, P. R. of China

²Beijing Computational Science Research Center, 3 Heqing Road, Beijing 100084, P. R. of China

Motivated by recent experiments of successfully carving out stable carbon atomic chains from graphene we investigate a device structure of a carbon chain connecting two zigzag graphene nanoribbons with highly tunable spin-dependent transport properties. Our calculation based on the non-equilibrium Green's function approach combined with the density functional theory shows that the transport behavior is sensitive to the spin configuration of the leads and the bridge position in the gap. A bridge in the middle gives an overall good coupling except for around the Fermi energy where the leads with anti-parallel spins create a small transport gap while the leads with parallel spins give a finite density of states and induce an even-odd oscillation in conductance in terms of the number of atoms in the carbon chain. On the other hand, a bridge at the edge shows a transport behavior associated with the spin-polarized edge states, presenting sharp pure α -spin and β -spin peaks beside the Fermi energy in the transmission function. This makes it possible to realize on-chip interconnects or spintronic devices by tuning the spin state of the leads and the bridge position.

I. INTRODUCTION

Carbon based nanostructures, especially, quasi-1D structures like carbon nanotubes (CNTs) and, recently, graphene nanoribbons (GNRs), are playing more and more important role in the development of nanoelectronics,¹ possibly leading to an era of carbon-based electronics. The practical application of CNTs is, however, limited by the challenge in controlling experimentally their diameter and chirality which control whether they are metallic or semiconducting. Different from CNTs, the electronic properties of GNRs are determined by their edge geometry and width and have shown promise for future generation of transistor.²⁻¹⁰ Zigzag-edged GNRs (ZGNRs) are particularly intriguing because of their spin-polarized edge states which are localized around the two edges. The resulting spin-dependent transport may make them promising candidates for applications in spintronics. In narrow ZGNRs with n zigzag carbon chains (denoted by n -ZGNRs, $n \lesssim 32$) the anti-parallel spin configuration is the ground state, which is slightly more favorable in energy than the parallel-spin one, while in wider n -ZGNRs ($n \gtrsim 32$) the two spin configurations are both possible to exist due to the negligible interaction between the two edge states.¹¹ Even in narrow ZGNRs, the small energy difference makes it possible to change the ground state from anti-parallel spins to parallel spins by applying a magnetic or electric field.¹¹

Recently, an interesting progress related to graphene is the successful fabrication of free-standing linear carbon atomic chains carved out from a graphene sheet by high-energy electron beam,¹²⁻¹⁴ which is found stable and is connected by sp^2 bonding. Unlike CNTs and GNRs, a carbon atomic chain has no chirality and width. Therefore, it provides an ideal transport channel for molecular devices. Experimentally, a carbon chain made in this way can be used as an on-chip device with the advantage of the perfect sp^2 connection to the leads already set. This is in striking contrast to the situation in conventional molecular electronics using metal electrodes where a well-defined molecule-lead contact with a good re-

produceability is a big challenge.¹⁵⁻¹⁷ For the miniaturization of the whole device, the two graphene leads can be cut to form GNRs. Theoretically, the device structure of a carbon chain connecting two ZGNR leads is particularly interesting since it combines the simple transport channel with the rich electronic properties of ZGNRs via the perfect sp^2 contact. Its transport properties can be artificially tailored to realize different functionalities, as shown in this work. First, the tunable spin state of the leads can be used to control the density of states at the Fermi energy, giving either a large or zero equilibrium conductance (switch). Second, the atomic thin bridge can be used to explore the locally spin-polarized edge states, implying that the transport behavior will be sensitive to the position of the bridge. This may be used to realize selectively the functionality of either on-chip interconnects or spintronics.

So far, the conductance of carbon chains connected to different types of electrodes have recently been studied by several research groups¹⁸⁻²⁶ but how it behaves is still an open problem depending on the nature of the electrode used. Among these work, a calculation²⁶ of spin-dependent transport was reported for a junction with very narrow ZGNR leads connected via a spin-polarized 5-member ring which is, however, unlikely to be carved out directly from a graphene sheet and is probably unstable due to the unpaired p_z electron without doping.²⁷

Recently Shen *et al* reported a theoretical calculation for carbon chain-ZGNR junctions with very narrow ZGNR leads but ignoring totally the spin freedom.²⁸ An interesting finding from their calculation is that the equilibrium conductance shows an even-odd oscillation with regard to the number of atoms in the carbon chain²⁸: A chain with an odd number of atoms will have a larger conductance than one with an even number of atoms. This even-odd behavior is due to the very sharp peak in the transmission function at the Fermi energy, whose origination was not understood clearly and was ascribed to the edge states of the leads. However, if one takes the spin freedom into account, this even-odd behavior will totally disappear for the ground state since the anti-parallel spins will create a band gap in the leads.

Another recent work about transport properties of carbon chain-GNR junctions was reported by Zanolli *et al.*,²⁹ in which the spin freedom was taken into account. In their calculation wider GNR leads are considered and a carbon chain is connected right in the middle of the gap. It was found that the spin freedom has a significant effect. Especially, an odd-numbered carbon chain bridge is found to be spin-polarized by itself while an even-numbered one is not. This calculation showed that an odd-numbered carbon chain combined with parallel-spin leads can give a large spin-polarized equilibrium conductance due to the peaks in the transmission function around the Fermi energy. This result implies that these peaks are not associated with the edge states because the bridge is in the middle and far away from the edges though their origination was unclear.

Despite these previous studies, a full understanding about the transport properties of carbon chain-ZGNR junctions is still lacking, especially the effect from the bridge position and its combination with the spin configuration and width of the leads, as well as the underlying physics leading to the transport behavior. In this work, we investigate the spin-dependent electron transport of carbon chain-ZGNR junctions by performing first-principles calculations based on the non-equilibrium Green's function (NEGF) approach combined with the density functional theory (DFT).^{30,31} We study systematically the effects from all the factors mentioned above. Our calculation shows that the bridge position combined with the spin freedom of the leads dominates the transport behavior. The underlying physics leading to this transport behavior is fully analyzed by investigating the space-resolved density of states (DOS). The present work indicates that different functionalities can be achieved by changing the bridge position and the spin state of the leads: on-chip interconnects can be realized with a bridge connected in the middle and a parallel spin configuration of the leads, which give a large equilibrium conductance, while a device for spintronics may be realized with a bridge connected at the edge, which gives a very high spin-polarization ratio.

II. COMPUTATIONAL DETAILS

We consider two widths for the ZGNR leads, consisting of 4 and 6 zigzag carbon chains, respectively (see Fig. 1). A carbon chain with 7 atoms is studied in details and a chain with 6 atoms is also calculated for showing the even-odd behavior in the equilibrium conductance. For the junction with the 4-ZGNR leads, the carbon chain is connected at two positions, one in the middle (M1-bridge) and the other at the edge (E-bridge). For the junction with the 6-ZGNR leads, three bridge positions are considered: in the right middle (M2-bridge), in the near middle (M1-bridge), and at the edge (E-bridge), respectively, (see Fig. 1).

Each edge of the two ZGNR leads has two possible spin states, α - or β -spin. In this work, we consider two spin configurations for the leads. In one configuration, both the left and right leads are in anti-parallel spin state with the top edge being α -spin and the bottom edge being β -spin (labeled by

$(\alpha\beta, \alpha\beta)$), which is the ground state of the narrow ZGNR lead. In the other, the two leads are in parallel-spin state with all the four edges being α -spin (labeled by $(\alpha\alpha, \alpha\alpha)$), which is possible under a magnetic field and/or for wider ZGNR leads. Our calculation will show that the effect from the width of the lead is quite small and therefore the narrow ZGNR leads considered will also reflect the major behavior of wider ones.

To investigate the electron transport through the carbon chain-ZGNR junctions we adopt the NEGF-DFT approach^{30,31} which combines the NEGF formula for transport with *ab initio* DFT calculation for electronic structure. In practice, the infinitely long 1-D system is divided into three parts: left lead, right lead, and device region containing the carbon chain plus enough ZGNR layers to accommodate the carbon chain-ZGNR interaction. The self-consistent Kohn-Sham Hamiltonian of the device region and the self-energies of two semi-infinite ZGNR leads are used to construct a single-particle Green's function from which the transmission coefficient at any energy is calculated. The conductance G

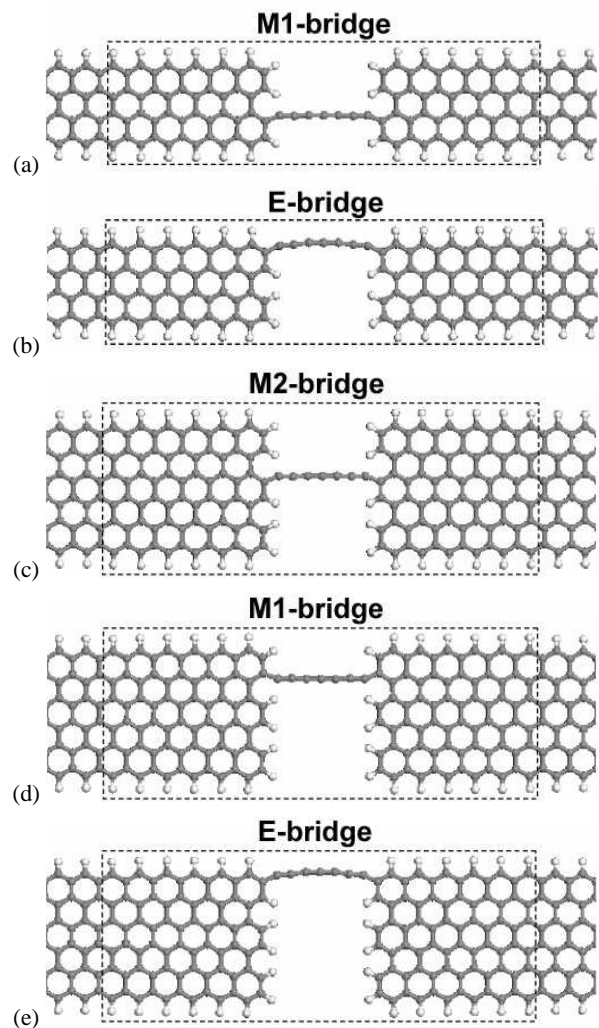


FIG. 1: Optimized atomic structures of the (4-ZGNR)-C₇-(4-ZGNR) and (6-ZGNR)-C₇-(6-ZGNR) junctions with different bridge positions: (a), (d) in the near middle (M1-bridge), (b), (e) at the edge (E-bridge), and (c) in the right middle (M2-bridge).

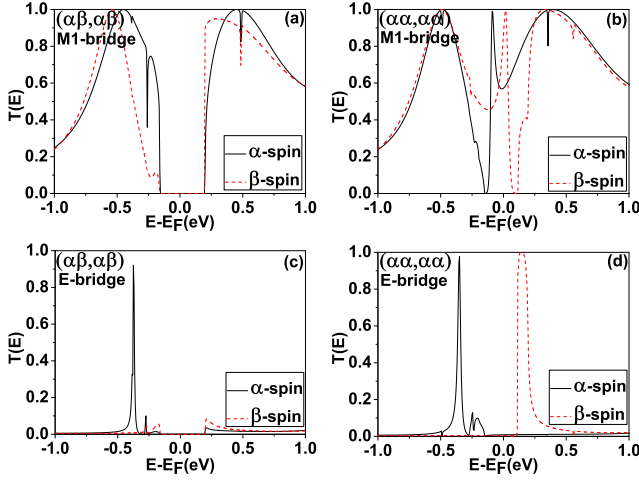


FIG. 2: Transmission functions of the (4-ZGNR)- C_7 -(4-ZGNR) junction. The first panel: M1-bridge connection in (a) $(\alpha\beta, \alpha\beta)$ and (b) $(\alpha\alpha, \alpha\alpha)$ spin configuration. The second panel: E-bridge connection in (c) $(\alpha\beta, \alpha\beta)$ and (d) $(\alpha\alpha, \alpha\alpha)$ spin configuration.

then follows from a Landauer-type relation. The computational techniques have been described in details previously.³¹ Briefly, for the DFT electronic structure calculation, we use a numerical basis set to expand the wave function³²: A double zeta plus polarization basis set (DZP) is adopted for all atomic species. The local density approximation (LDA)³³ is used for the electron exchange and correlation and the optimized Troullier-Martins pseudopotentials³⁴ are used for the atomic cores. The atomic structure of the junctions including the carbon chain-ZGNR separation are fully optimized by minimizing the atomic forces on the atoms to be smaller than 0.02 eV/\AA .

III. RESULT AND DISCUSSION

A. Effects of spin and bridge position

The calculated transmission functions for the (4-ZGNR)- C_7 -(4-ZGNR) and (6-ZGNR)- C_7 -(6-ZGNR) junctions are plotted in Figs. 2 and 3, respectively. The first thing to note is that the transmission function depends very significantly on the spin configuration of the leads and the position of the carbon chain bridge in the gap. When the bridge is positioned around the middle range of the gap (M2- and M1-bridge) the transmission function is overall broad in the energy window $[-1, 1] \text{ eV}$, indicating a strong coupling between the carbon chain and the ZGNR leads. For the anti-parallel spin configuration $(\alpha\beta, \alpha\beta)$ there is a small transport gap around the Fermi energy (Figs. 2 (a) and 3 (a), (c)) while for the parallel spin configuration $(\alpha\alpha, \alpha\alpha)$ there are sharp resonance peaks there (Figs. 2 (b) and 3 (b), (d)). The transport gap in the case of $(\alpha\beta, \alpha\beta)$ is due to the band gap created by the anti-parallel spins in the leads, as shown in Figs. 4 (a) and (c). Note that this band gap decreases slowly with the increasing width of the ribbon and so is the transport gap: 0.37 and 0.35 eV for the 4-ZGNR and 6-ZGNR junctions, respectively. In the case

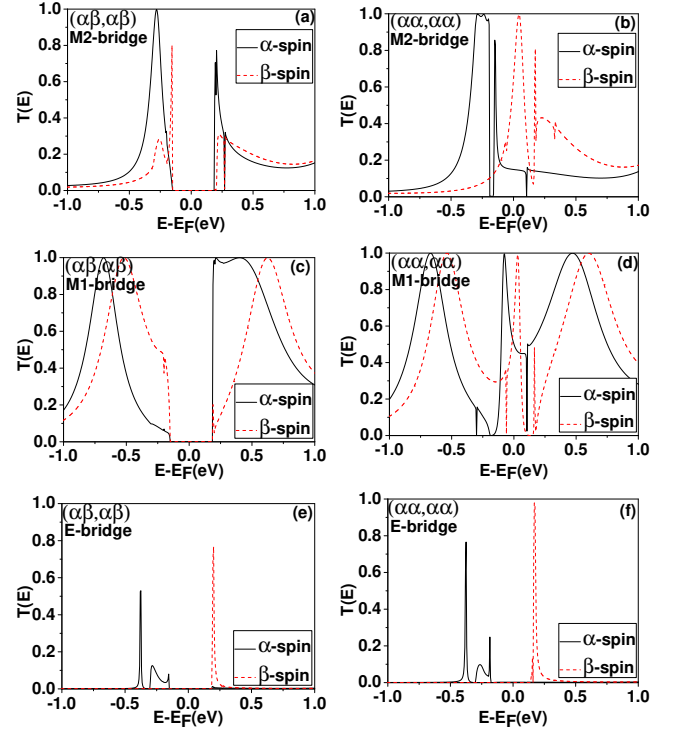


FIG. 3: Transmission functions of the (6-ZGNR)- C_7 -(6-ZGNR) junction. The first panel: M2-bridge connection in (a) $(\alpha\beta, \alpha\beta)$ and (b) $(\alpha\alpha, \alpha\alpha)$ spin configuration. The second panel: M1-bridge connection in (c) $(\alpha\beta, \alpha\beta)$ and (d) $(\alpha\alpha, \alpha\alpha)$ spin configuration. The third panel: E-bridge connection in (e) $(\alpha\beta, \alpha\beta)$ and (f) $(\alpha\alpha, \alpha\alpha)$ spin configuration.

of $(\alpha\alpha, \alpha\alpha)$, the parallel spin state causes a band crossing at the Fermi energy as shown in Figs. 4 (b) and (d), providing an finite DOS around the Fermi energy in the leads. The coupling of this finite DOS to the electronic states in the carbon chain gives rise to the sharp resonance peaks around the Fermi energy (see further discussion later).

On the other hand, when the carbon chain bridge is positioned at the edge of the gap (E-bridge) the transmission function becomes very sharp peaks in the energy window $[-1, 1] \text{ eV}$ (Figs. 2 (c), (d), and 3 (e), (f)), indicating an overall weak chain-lead coupling. Furthermore, around the Fermi energy the α - and β -spin peaks are now separated largely from each other, making the transport at the Fermi energy is also blocked for the $(\alpha\alpha, \alpha\alpha)$ spin configuration (Figs. 2 (d) and 3 (f)).

Being consistent with the previous calculation adopting wider ZGNR leads,²⁹ our calculation shows that the C_7 chain is spin-polarized by itself.³⁵ This leads to the spin-polarized transport even when the carbon chain is connected in the right middle (i.e., M2-bridge, see Fig.3 (b)). However, the present calculation further shows that the resulting spin-polarized transport is significantly modulated by the bridge position. For example, in the case of $(\alpha\alpha, \alpha\alpha)$ the splitting between the α - and β -spin peaks and also the spin polarization ratio around the Fermi energy varies largely with the bridge position (see Fig.3 (b) vs (d)) due to the interaction with the edge states (see further discussion later).

As for the effect from the width of the lead, one can see that

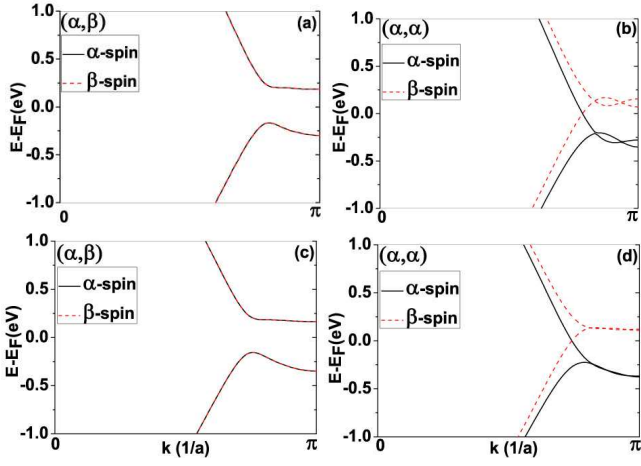


FIG. 4: The first panel: Band structure of a 4-ZGNR in (a) (α, β) and (b) (α, α) spin configuration. The second panel: Band structure of a 6-ZGNR in (c) (α, β) and (d) (α, α) spin configuration.

for the same M1-bridge connection the overall effect in the transmission function is not significant and does not change the qualitative result when the width of the leads is increased from 4 to 6 zigzag chains: Fig. 2 (a) vs Fig. 3 (c) for $(\alpha\beta, \alpha\beta)$, and Fig. 2 (b) vs Fig. 3 (d) for $(\alpha\alpha, \alpha\alpha)$. Therefore, the results from the present calculation can be expected to be still qualitatively valid for junctions with wider ZGNR leads.

B. Analyses

Physically, the complicated spin-dependent transport behavior and the very significant effect from the bridge position is related to the spin-polarized edge states and their spatial distribution in the leads. To understand the results and provide an insight into the physics underlying, we study the spin-polarized projected density of states (PDOS) for the leads and the local density of states (LDOS) for the characteristic peaks in the transmission function of the junctions.

In Fig. 5 we show the spin-polarized PDOS for the edge and bulk regions of an infinite long 6-ZGNR. In the bulk region of the ribbon (Figs. 5 (a) and (b)) the bulk states provide a finite DOS in the whole energy window except for that around the Fermi energy where a gap appears for (α, β) because of the band gap shown in Fig. 4 (c), while a finite DOS still exists for (α, α) due to the band crossing shown in Fig. 4 (d). When the bridge is positioned in the middle region of the gap the finite DOS apart from the Fermi energy couples with the states in the bridge, leading to the very broad transmission function shown in Figs. 3 (a) - (d). To show this more clearly, we plot in Fig. 6 the LDOS for the energy around -0.68 eV in Figs. 3 (a) and (c), respectively. It can be seen that in both cases the LDOS spreads out through the whole junction and distributes quite evenly in the leads, indicating that it is associated with the bulk states. In the case of (α, α) the finite DOS around the Fermi energy couples with the spin-polarized states in the bridge (their PDOS is plotted in Figs. 5 (e) and (f)) and gives rise to the resonance peaks around the Fermi

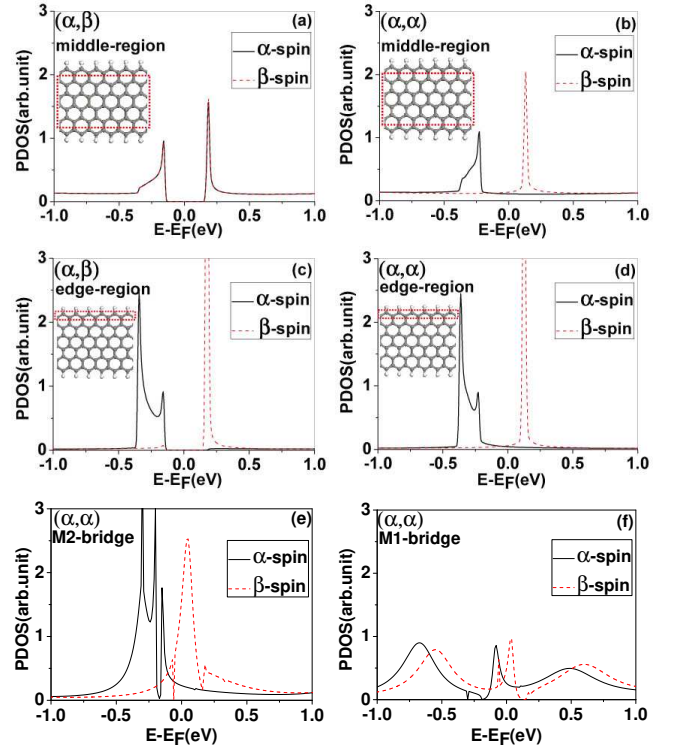


FIG. 5: The first panel: PDOS projected on the bulk region of a 6-ZGNR for (a) (α, β) and (b) (α, α) spin configuration. The second panel: PDOS projected on the edge region of a 6-ZGNR for (c) (α, β) and (d) (α, α) spin configuration. The third panel: PDOS projected on the C_7 chain in the (6-ZGNR)- C_7 -(6-ZGNR) junction with (e) M2-bridge and (f) M1-bridge connection in the $(\alpha\alpha, \alpha\alpha)$ spin configuration.

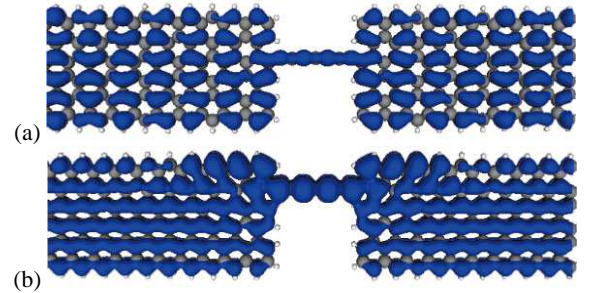


FIG. 6: (a) and (b): LDOS of the α -spin component around -0.68 eV in Fig.3 (a) and (c), respectively.

energy in the transmission function (Figs. 3 (b) and (d)). To show the nature of these resonance peaks we plot their LDOS for the β -spin component in Figs. 7 (a) and (b) for the M2- and M1-bridge connections, respectively. One can see that when the bridge is positioned in the right middle (M2-bridge) the LDOS has large contribution from the bridge region and is distributed evenly throughout the leads, indicating that it is a result of the coupling between the states in the bridge and the bulk states in the leads. When the bridge is closer to the edge (M1-bridge) now the LDOS has also large contribution from the edge states within the scattering region, indicating an interaction between the spin-polarized bridge states and the edge

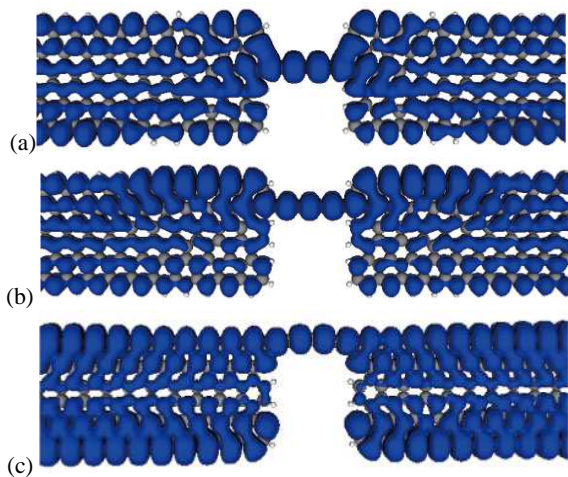


FIG. 7: (a), (b), (c): LDOS of the β -spin peaks around the Fermi energy (0.05, 0.03, and 0.17 eV, respectively) in Fig.3 (b), (d), and (f), respectively.

states, which modulates the spin-polarized transport behavior of the junction around the Fermi energy (see Fig.3 (b) vs (d)).

On the other hand, for the zigzag chain of the edge (Figs. 5 (c) and (d)) the PDOS reflects essentially the edge state which has two sharp peaks beside the Fermi energy, i.e., the occupied α -spin and unoccupied β -spin states, respectively, placing a near-zero DOS elsewhere. Consequently, when the bridge is positioned at the edge it mainly couples with these edge states, leading to the transmission function with only very sharp peaks corresponding to the edge states, as shown in Figs. 3 (e) and (f). The LDOS of the β -spin peak in Fig. 3 (f) plotted in Figs. 7 (c) shows that the transport is indeed along the two edges. In this case, even for the $(\alpha\alpha, \alpha\alpha)$ spin configuration the transport around the Fermi energy is also nearly blocked. Note that unlike the transport gap created by the anti-parallel spins in $(\alpha\beta, \alpha\beta)$ case, this transport gap between the α - and β -spin components actually increases from the 4-ZGNR to the 6-ZGNR junction (0.26 and 0.33eV, respectively). This is because the $\alpha - \alpha$ spin interaction in the narrow 4-ZGNR lead induces extra dispersions of the edge states, as shown in Fig. 4 (b) vs (d).

The broad and very narrow peaks in the transmission function reflect the overall coupling strength between the carbon chain and the ZGNR leads. It is interesting to note that the best coupling is given by neither the bridge at the edge (E-bridge) nor the bridge right in the middle (M2-bridge) but the one positioned in between (M1-bridge). This is evident in the LDOS shown in Fig. 6 where the M1-bridge gives a remarkably larger LDOS around the bridge and contact region than the M2-bridge does. The result is a much larger transmission coefficient around -0.68 eV in Fig. 3 (c) than that in Fig. 3 (a).

C. Even-odd behavior

Finally, we would like to discuss the even-odd behavior in the equilibrium conductance found previously in the spin-unpolarized calculation.²⁸ This calculation shows that short

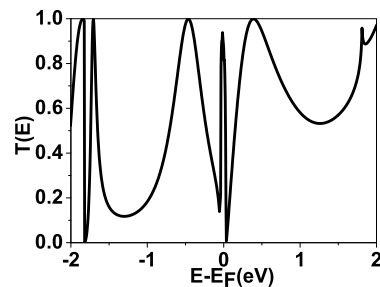


FIG. 8: Transmission function of the spin-unpolarized (4-ZGNR)- C_7 -(4-ZGNR) junction.

carbon atomic chains with an odd number of atom will give a significantly larger equilibrium conductance than those with an even number of atom. According to the present calculation, however, the spin freedom must be taken into account in reaching this conclusion. To have a direct comparison, we also perform spin-unpolarized calculation for the narrow 4-ZGNR junction with the M1-bridge and plot the result in Fig. 8, which is basically the same as obtained in Ref.²⁸ The very sharp peak at the Fermi energy is the origination of the even-odd oscillation in conductance, which was ascribed to the edge states.²⁸ The present spin-polarized result in Fig. 2 shows that this peak around the Fermi energy only exists in the case of $(\alpha\alpha, \alpha\alpha)$ with the M1-bridge connection (see Fig. 2 (b)) but now having a small splitting between the α - and β -spin components. In the case of $(\alpha\beta, \alpha\beta)$ the equilibrium conductance is zero simply because the band gap created by the anti-parallel spins in the leads (see Fig. 2 (a)). Additionally, for the E-bridge connection even in the case of $(\alpha\alpha, \alpha\alpha)$ the equilibrium conductance is also nearly zero because of the large splitting between the α - and β -spin components (see Fig. 2 (d)). For the wider (6-ZGNR)- C_7 -(6-ZGNR) junction, the result is similar – the sharp peaks around the Fermi energy only appear in the case of $(\alpha\alpha, \alpha\alpha)$ and only when the bridge is positioned around the middle region (see Fig. 3).

The present spin-polarized calculation shows that, as can be seen in Figs. 7 (a) and (b), the large resonance peaks at the Fermi energy is not originated from the edge states, but comes from the coupling between the finite DOS in the leads due to the band crossing and the states in the bridge whose PDOS is given in Figs. 5 (e) and (f) showing a large DOS around the Fermi energy for the C_7 chain. Since in this case the coupling to the leads is determined by the states in the carbon chain, the resulting equilibrium conductance will be sensitive to its electronic state which may be affected significantly by the number of atoms in the chain. As was found in Ref.,²⁸ an even or odd number of atoms in the carbon chain will result in different C-C bond-length distribution due to the Peils transition effect and therefore gives quite different electronic states.

In order to make this issue more clear, we calculate the transmission function of a (6-ZGNR)- C_6 -(6-ZGNR) junction with the M2-bridge connection for the $(\alpha\alpha, \alpha\alpha)$ spin configuration. The result and the PDOS projected on the C_6 chain are plotted in Figs. 9 (a) and (b), respectively. The small DOS at Fermi energy for the C_6 chain shows the the coupling between the lead and the carbon chain is very weak, resulting a

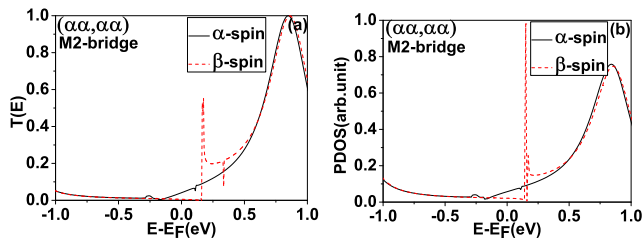


FIG. 9: (a) Transmission function of the (6-ZGNR)-C₆-(6-ZGNR) junction in the ($\alpha\alpha, \alpha\alpha$) spin configuration and with the M2-bridge connection. (b) PDOS projected on the C₆ chain of the junction.

much smaller equilibrium conductance compared with the C₇ junction. The consequence is an even-odd oscillation in the equilibrium conductance in terms of the number of atoms in the carbon chain.

IV. SUMMARY

In summary, motivated by recent experiments of successfully carving out stable carbon atomic chains from graphene, we have studied the spin-dependent electron transport through carbon atomic chains connecting two zigzag graphene nanoribbons by using the non-equilibrium Green's function approach combined with the density functional theory calculation. The effects on the transport from different spin configurations of the leads, different positions of the bridge connection, and the width of the leads are investigated.

It was found that the bridge position combined with the spin freedom dominate the transport properties. A bridge connection in the middle will give an overall good coupling and

transparency because of the strong coupling between the bulk states in the leads and those in the atomic chain, except for the energies around the Fermi energy where the lead with anti-parallel spins creates a transport gap while the lead with parallel spins give a finite density of states because of its band crossing. The coupling between this finite density of states and the states in the carbon chain gives rise to a large (for odd-numbered chains) or a small (for even-numbered chains) equilibrium conductance for both the α - and β -spin components, inducing an even-odd oscillation in the equilibrium conductance. On the other hand, a bridge at the edge leads to a transport behavior associated with the edge states, showing only sharp pure α -spin and β -spin peaks beside the Fermi energy with a near zero equilibrium conductance.

Our calculation reveals that a functional device for on-chip interconnects can be realized by a bridge connection in the near middle (M1-bridge), which gives a large equilibrium conductance when the leads are in the parallel-spin configuration. This spin configuration together with a bridge connected not at the edge may also be used to realize spintronic device with a moderate spin-polarization ratio. On the other hand, a functional spintronic device with a very high spin polarization ratio may be realized by a bridge connection at the edge with a small gate voltage shifting the Fermi energy to the energy of the pure α - or β -spin peak.

Acknowledgments

This work was supported by Shanghai Pujiang Program under Grant No. 10PJ1410000 and by the National Natural Science Foundation of China under Grant No. 11174220 as well as by the MOST 973 Project 2011CB922204.

* Corresponding author, E-mail: shke@tongji.edu.cn

¹ P. Avouris, Z. Chen, and V. Perebeinos, *Nat. Nanotechnol.* **2**, 605 (2007).

² K. Nakada, M. Fujita, G. Dresselhaus, and M. S. Dresselhaus, *Phys. Rev. B* **54**, 17954 (1996).

³ A. H. Castro Neto, F. Guinea, N. M. R. Peres, K. S. Novoselov, and A. K. Geim, *Rev. Mod. Phys.* **81**, 109 (2009).

⁴ A. Geim and K. Novoselov, *Nat. Mater.* **6**, 183 (2007).

⁵ M. Y. Han, B. Özyilmaz, Y. Zhang, and P. Kim, *Phys. Rev. Lett.* **98**, 206805 (2007).

⁶ Y.-W. Son, M. L. Cohen, and S. G. Louie, *Phys. Rev. Lett.* **97**, 216803 (2006).

⁷ N. M. R. Peres, A. H. Castro Neto, and F. Guinea, *Phys. Rev. B* **73**, 195411 (2006).

⁸ X. Wang, Y. Ouyang, X. Li, H. Wang, J. Guo, and H. Dai, *Phys. Rev. Lett.* **100**, 206803 (2008).

⁹ Q. Yan, B. Huang, J. Yu, F. Zheng, J. Zang, J. Wu, B.-L. Gu, F. Liu, and W. Duan, *Nano Lett.* **7**, 1469 (2007).

¹⁰ B. Standley, W. Bao, H. Zhang, J. Bruck, C. N. Lau, and M. Bockrath, *Nano Lett.* **8**, 3345 (2008).

¹¹ Y. Son, M. Cohen, and S. Louie, *Nature* **444**, 347 (2006).

¹² J. Meyer, C. Girit, M. Crommie, and A. Zettl, *Nature* **454**, 319 (2008).

¹³ A. Chuvilin, J. Meyer, G. Algara-Siller, and U. Kaiser, *New J.*

Phys. **11**, 083019 (2009).

¹⁴ C. Jin, H. Lan, L. Peng, K. Suenaga, and S. Iijima, *Phys. Rev. Lett.* **102**, 205501 (2009).

¹⁵ H. Basch, R. Cohen, and M. Ratner, *Nano Lett.* **5**, 1668 (2005).

¹⁶ L. Venkataraman, J. Klare, I. Tam, C. Nuckolls, M. Hybertsen, and M. Steigerwald, *Nano Lett.* **6**, 458 (2006).

¹⁷ S.-H. Ke, H. Baranger, and W. Yang, *J. Chem. Phys.* **122**, 074704 (2005).

¹⁸ S. Tongay, R. Senger, S. Dag, and S. Ciraci, *Phys. Rev. Lett.* **93**, 136404 (2004).

¹⁹ N. Lang and P. Avouris, *Phys. Rev. Lett.* **84**, 358 (2000).

²⁰ Y. Zhou, X. Zheng, Y. Xu, and Z. Zeng, *J. Phys.: Condens. Matter* **20**, 045225 (2008).

²¹ M. Brandbyge, J. Mozos, P. Ordejon, J. Taylor, and K. Stokbro, *Phys. Rev. B* **65**, 165401 (2002).

²² B. Larade, J. Taylor, H. Mehrez, and H. Guo, *Phys. Rev. B* **64**, 075420 (2001).

²³ Y. Wei, Y. Xu, J. Wang, and H. Guo, *Phys. Rev. B* **70**, 193406 (2004).

²⁴ K. Khoo, J. Neaton, Y. Son, M. Cohen, and S. Louie, *Nano Lett.* **8**, 2900 (2008).

²⁵ H. Cheraghchi and K. Esfarjani, *Phys. Rev. B* **78**, 085123 (2008).

²⁶ J. Fürst, M. Brandbyge, and A. Jauho, *Europhys. Lett.* **91**, 37002 (2010).

- ²⁷ S.-H. Ke, H. Baranger, and W. Yang, *Phy. Rev. Lett.* **99**, 146802 (2007).
- ²⁸ L. Shen, M. Zeng, S. Yang, C. Zhang, X. Wang, and Y. Feng, *J. Am. Chem. Soc.* (2010).
- ²⁹ Z. Zanolli, G. Onida, and J. Charlier, *ACS nano* **4**, 5174 (2010).
- ³⁰ S. Datta, *Electronic Transport in Mesoscopic Systems* (Cambridge University Press, Cambridge, England, 1995).
- ³¹ S. Ke, H. Baranger, and W. Yang, *Phys. Rev. B* **70**, 085410 (2004).
- ³² J. Soler, E. Artacho, J. Gale, A. García, J. Junquera, P. Ordejón, and D. Sánchez-Portal, *J. Phys.: Condens. Matter.* **14**, 2745 (2002).
- ³³ D. M. Ceperley and B. J. Alder, *Phys. Rev. Lett.* **45**, 566 (1980).
- ³⁴ N. Troullier and J. L. Martins, *Phy. Rev. B* **43**, 1993 (1991).
- ³⁵ The converged spin-polarized electronic states in the carbon chain are sensitive to the choice for the initial spins of the atoms at the edges of the leads. Therefore these initial spins must be chosen carefully otherwise it may be converged to the spin-unpolarized state. The total energy of the system shows that the spin-polarized state is the ground state.